

Influence of Ba content on grain size and dynamics of crystallization in barium ferrite thin films

Yingjian Chen, David E. Laughlin, Xiaoding Ma, and Mark H. Kryder
Data Storage Systems Center, Carnegie Mellon University, Pittsburgh, Pennsylvania 15213

The effects of Ba content on the dynamics of the crystallization process, which ultimately determines the grain size, were studied in barium ferrite thin films. Rapid thermal annealing was used to crystallize the amorphous as-deposited barium ferrite films. The annealing time and temperature dependent crystalline volumes were determined from the magnetization of the films, and were analyzed by means of the Johnson–Mehl–Avrami relation. Microstructural studies showed that the films with higher Ba content had higher nucleation rates and lower growth rates; consequently, they had finer grain size and smaller grain aspect ratio. Magnetic measurements showed that the higher Ba content films also had higher coercivities and smaller magnetic switching volumes. © 1997 American Institute of Physics. [S0021-8979(97)36608-0]

I. INTRODUCTION

Barium hexaferrite thin film media are attractive candidates for ultrahigh density over-coat free magnetic recording. In order to achieve this goal, magnetic grains as small as 100 Å are necessary to obtain reasonable signal to noise ratio (SNR) in recording at high areal density.¹

Barium ferrite thin films, sputtered onto substrates at room temperature, are amorphous and nonmagnetic. The amorphous-to-crystalline phase transformation to a magnetic film is achieved by annealing at temperatures as high as 800 °C and is an important step. Many microstructural properties such as grain size as well as many magnetic characteristics are dependent on this thermodynamic transition process. Parker *et al.* studied this process in barium ferrite grown on single crystal sapphire substrates.² In this study, we have investigated how microstructure may be controlled in barium ferrite thin films deposited on amorphous oxidized silicon substrates. The nucleation and growth of crystallites were studied by using both microstructural and magnetic measurements.

II. EXPERIMENTAL PROCEDURES

Barium ferrite thin films of 1000 Å thickness were deposited from two targets having different Ba contents onto oxidized silicon substrates. A rf sputtering power of 100 W was used in a Leybold Z-650 sputtering system. Target 1 contains ~18 weight percent (wt%) of BaO, whereas target 2 has ~23 wt% of BaO, determined using energy dispersive x-ray fluorescence (EDXRF). The wt% of BaO in the deposited films is 4%–5% less than that in the targets. The amorphous films were then rapidly thermally annealed (RTA) at temperatures of 780, 800, and 820 °C for various annealing times to achieve different degrees of crystallization.

The microstructure of the films was studied using an atomic force microscope (AFM). The films were briefly etched before the AFM measurements in order to enhance their topographical features. A JEOL 120cx transmission electron microscope (TEM) was also used to confirm that the topographical features measured by AFM were representative of the grain size.

The in-plane magnetic properties of the films were studied on an alternating gradient magnetometer (AGM). M_s and H_c were determined from the hysteresis loops of the films.

The switching volume V_{sw} was obtained from the “waiting time” measurement³ by using the time dependence of coercivity⁴

$$H_c(t') = H_a \left\{ 1 - \left[\frac{2k_B T}{H_a M_s V_{sw}} \ln \left(\frac{A t'}{0.693} \right) \right]^{1/2} \right\}, \quad (1)$$

where t' is the time for the magnetization to decay to zero at an applied field H in the vicinity of the coercivity. The constant A is an attempt frequency taken to be 10^9 . The fitting parameters V_{sw} and the anisotropy field H_a were determined by fitting Eq. (1) to measurements of t' for a given applied field [$H_c(t')$].

III. RESULTS

The topographic grain structures as measured on the AFM in the low Ba content barium ferrite films at a temperature of 820 °C, and at annealing times of 10 and 20 s, are shown in Fig. 1. It is observed that the barium ferrite grains are elongated along one of their in-plane directions. With the increase of annealing time, the grains grew further along these directions and more grains were formed. The growth stopped when the neighboring grains abutted one another.

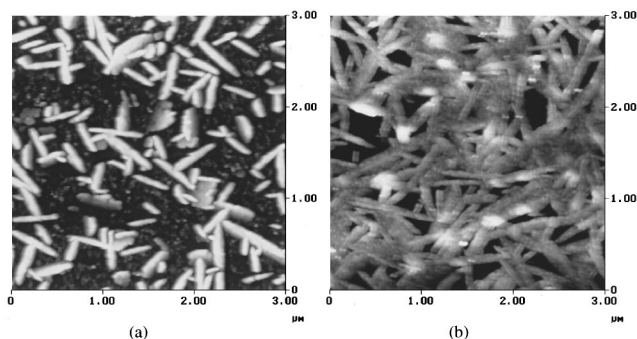


FIG. 1. AFM images ($3 \times 3 \mu\text{m}$) of low Ba content films after annealing at 820 °C for (a) 10 s and (b) 20 s.

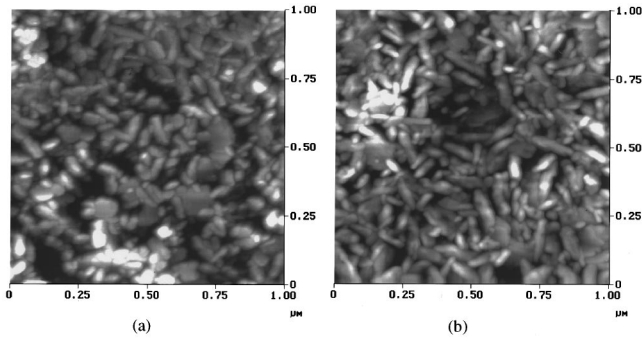


FIG. 2. AFM images ($1 \times 1 \mu\text{m}$) of high Ba content films after annealing at 820°C for (a) 8 s and (b) 14 s.

The nucleation rate R_N and the growth rate R_G were measured at early stages of crystallization when the nucleation and growth of grains took place independently of each other. R_N of about 9 grains/s in an area of $3 \times 3 \mu\text{m}$ and R_G of about 69 nm/s along their acicular directions were estimated from Fig. 1.

The transformation in the higher Ba content barium ferrite films at a temperature of 820°C is shown in Fig. 2. The nucleation rate in these films was found to be much higher than in the low Ba content films, and the growth rate was lower as indicated by the greater number of grains in the same area, and by the shorter grain dimensions. The values of R_N and R_G measured at different temperatures using this method for both sets of films are listed in Table I. The average final grain size of the high Ba content films was about $500 \text{ \AA} \times 1500 \text{ \AA}$, much smaller than that of the low Ba content films, which was about $1500 \text{ \AA} \times 1 \mu\text{m}$ with a higher average grain aspect ratio of 6 to 8. TEM images of the films annealed at 800°C for 12 and 30 s, respectively, are shown in Fig. 3 and indicate good agreement between the grain size and the measured AFM topographical features.

As also shown in Table I, the activation energies for the nucleation ΔH_N and for the growth ΔH_G were determined from the nucleation and the growth rate by means of the Arrhenius relation,⁵ $R_N \propto \exp(-\Delta H_N/k_B T)$; $R_G \propto \exp(-\Delta H_G/k_B T)$. The high Ba content films were found to have a lower energy barrier for nucleation, but a higher energy barrier for growth, as reflected by their higher nucleation rate and lower growth rate, respectively.

The annealing time dependencies of the saturation magnetization of the films at isothermal annealing temperatures of 780, 800, and 820°C are shown in Fig. 4. The value of

TABLE I. Nucleation, growth rate, and activation energies.

T ($^\circ\text{C}$)	Growth rate R_G (nm/s)	Nucleation rate R_N (grains/s/ $25 \mu\text{m}^2$)	ΔH_G (eV/atom)	ΔH_N (eV/atom)
Target 1, low Ba content				
780	20	2.9		
800	37	14	1.71	2.98
820	69	25		
Target 2, high Ba content				
780	4.2	84.2		
800	7.2	167	1.96	2.12
820	17.5	390		

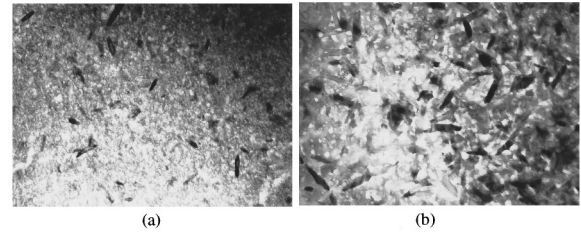


FIG. 3. TEM bright-field images (about $1.4 \times 1 \mu\text{m}$) of high Ba content films after annealing at 800°C for (a) 12 s and (b) 30 s.

M_s increases asymptotically to 280–300 emu/cc with annealing time ($M_s t$ value of 1.1 memu/cm²). To evaluate the crystallized fractions of each film at different annealing times, the value of M_s relative to that after a long term anneal was used. The curves were analyzed using the Johnson–Mehl–Avrami (JMA) kinetic equation⁶

$$x(t) = 1 - \exp(-K_T t^n) = 1 - \exp\left[-\left(\frac{t}{\tau}\right)^n\right], \quad (2)$$

where $x(t)$ is the normalized crystalline volume, K_T and τ are temperature dependent kinetic constants, and n is the Avrami exponent, which is related to the transformation mechanism. The n value for a linear time dependent nucleation and two-dimensional (2D) growth is 3, whereas for a linear time dependent nucleation and one-dimensional (1D) growth it is 2.

Fitting the curves before they reach their asymptotic values resulted in values of n of about 3 for the high Ba content films. On the other hand, $n=2$ gave a reasonable fit to the curves corresponding to lower Ba content films. The results of the fitting are shown in Table II. The activation energy for transformation ΔH_Q is again determined from the Arrhenius relation.^{5,7}

The annealing time dependencies of H_c are shown in Fig. 5. The results indicate that H_c saturates earlier than M_s does. The Ba rich films have higher final H_c values (~ 5000 Oe) than the low Ba content films (~ 3200 Oe).

The remanent squareness S and the coercivity square

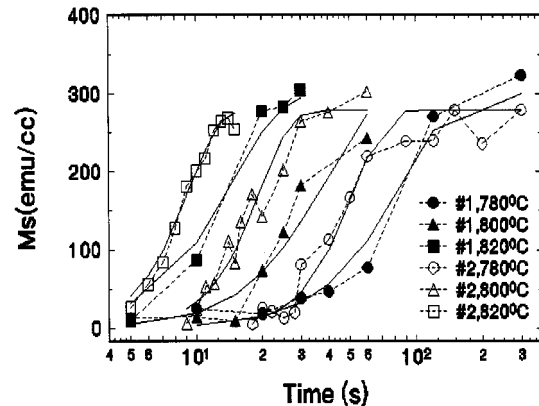


FIG. 4. Dependence of M_s on annealing time at different temperatures. The symbols represent experimental data and the solid lines represent fits to the JMA equation.

TABLE II. Fitting parameters in the Johnson-Mehl-Avrami equation.

T (°C)	M_s (emu/cc)	n	τ (s)	K_T	ΔH_Q (eV/atom)
Target 1, low Ba content					
780	300	2	87.8	1.3×10^{-4}	4.9
800	300	2	38.5	6.8×10^{-4}	
820	300	2	14.9	4.5×10^{-3}	
Target 2, high Ba content					
780	280	3.04	52.3	5.8×10^{-6}	7.5
800	280	3.03	19.7	1.2×10^{-4}	
820	280	2.97	9.23	1.37×10^{-3}	

ness S^* in the fully crystallized films were 0.66 and 0.88, respectively, in the high Ba content films. They were 0.6 and 0.65 in the low Ba content films.

In the fully crystallized films, V_{sw} in the high Ba content films were found to be about 50% of those in the low Ba content films. The values of V_{sw} were much smaller than the average physical grain size in all films. V_{sw} of the high Ba content films was seen to increase at about the same rate as M_s with annealing time, as seen by comparing Figs. 4 and 6.

IV. DISCUSSION AND CONCLUSION

Barium ferrite films such as the films studied here have in-plane oriented magnetic easy axes, which are also the c axes of the crystallites. It is known that barium ferrite has slow growth along the c axis, and fast growth in the ab plane.⁸ It is thus expected that barium ferrite would show rapid 2D growth. However, the growth perpendicular to the film is constrained by the film surfaces. According to the growth rate given in Table I, only 2–3 s are required for the crystallites to grow to the film thickness of 1000 Å at an annealing temperature of 800 °C in the low Ba content films. Such a short time is negligible in comparison to the annealing time window of 60 s. The growth in the low Ba content films was, therefore, predominantly 1D, while that in the Ba rich films which grew much more slowly remained 2D. As a result, the values of the Avrami exponent n should be 2 and 3 in the low and high Ba content films, respectively. These values are in agreement with the values shown in Table II.

EDXRF results showed that the low Ba content films sputtered from the slightly Ba rich target are almost stoichiometric

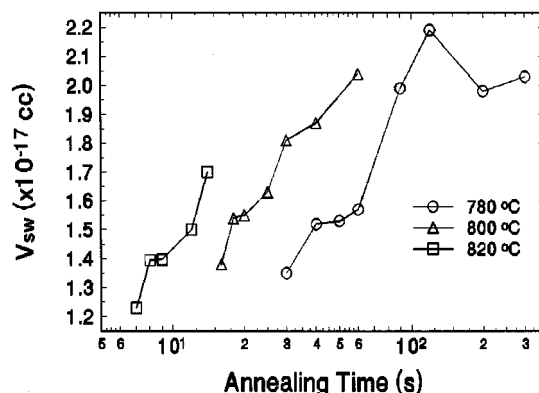


FIG. 6. Dependence of V_{sw} on annealing time at different temperatures in the high Ba content films.

metric $BaFe_{12}O_{19}$, whereas the higher Ba content films are about 5 wt% BaO rich. It is suggested that the reason for the higher growth rate in the low Ba content films is that crystallites in stoichiometric films grow more easily after nucleation, whereas the growth rate in the films with Ba content higher than stoichiometry may be limited by diffusion. On the other hand, the local Ba rich sites in the high Ba content films may provide more nucleation centers. This would explain why the activation energy for growth in the Ba rich films is about 0.25 eV/atom higher and that for nucleation is about 0.86 eV/atom lower. The final grain size and grain aspect ratio are the results of the competition between the nucleation and the growth. A higher nucleation rate and a lower growth rate result in finer grains with shorter grain aspect ratios as observed in the Ba rich films.

The much smaller V_{sw} than the grain size may be caused by incoherent rotation of magnetization.⁹ The incoherent rotation is expected to be more prominent in the larger and more acicular grains.¹⁰ The much lower H_c observed in the low Ba content films may also be due to this effect.¹¹

ACKNOWLEDGMENTS

The authors would like to thank Dr. J. K. Howard of IBM for many helpful discussions. This work was supported by the National Science Foundation under Grant No. ECD-8907068.

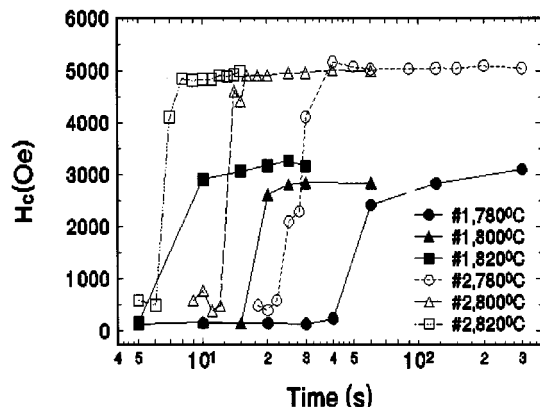


FIG. 5. Dependence of H_c on annealing time at different temperatures.

- ¹E. S. Murdock, R. F. Simmons, and R. Davidson, *IEEE Trans. Magn.* **MAG-28**, 3078 (1992).
- ²M. A. Parker, T. L. Hylton, K. R. Coffey, and J. K. Howard, *Mater. Res. Soc. Symp. Proc.* **280**, 625 (1993).
- ³R. W. Chantrell, G. N. Coverdale, and K. O'Grady, *J. Phys. D* **21**, 1469 (1988).
- ⁴M. P. Sharrock and J. T. McKinney, *IEEE Trans. Magn.* **MAG-17**, 3020 (1981).
- ⁵J. W. Christian, *The Theory of Transformation in Metals and Alloys* (Pergamon, Oxford, 1975), Chap. 3, pp. 77–92.
- ⁶M. Avrami, *J. Chem. Phys.* **7**, 1103 (1939); **8**, 212 (1940); **9**, 177 (1941).
- ⁷K. Lu, R. Luck, and B. Predel, *Acta Metall. Mater.* **42**, 2303 (1994).
- ⁸J. Smit and H. P. J. Wijn, *Ferrites* (Wiley, New York, 1959), Chap. 11, p. 227.
- ⁹Y. J. Chen, L. Tang, D. E. Laughlin, and M. H. Kryder, *IEEE Trans. Magn.* **32**, 3608 (1996).
- ¹⁰M. E. Schabes and N. Bertram, *IEEE Trans. Magn.* **MAG-25**, 3662 (1989).
- ¹¹E. Kneller and F. E. Luborsky, *J. Appl. Phys.* **34**, 656 (1963).